

# Metal/ $\text{Al}_2\text{O}_3$ - $\text{SiO}_2$ System Interface Investigations

N. Korobova\*, Deawha Soh\*\*

\*Combustion Problems Institute, Kazakhstan, \*\*Myongji University, Korea  
dwshoh@mju.ac.kr

*Abstract*— The packaging of the integrated circuits requires knowledge of ceramics and metals to accommodate the fabrication of modules that are used to construct subsystems and entire systems from extremely small components. Composite ceramics ( $\text{Al}_2\text{O}_3$  -  $\text{SiO}_2$ ) were tested for substrates. A stress analysis was conducted for a linear work-hardening metal cylinder embedded in an infinite ceramic matrix. The bond between the metal and ceramic was established at high temperature and stresses developed during cooling to room temperature. The calculations showed that the stresses depend on the mismatch in thermal expansion, the elastic properties, and the yield strength and work hardening rate of the metal. Experimental measurements of the surface stresses have also been made on a  $\text{Cu}/\text{Al}_2\text{O}_3$  -  $\text{SiO}_2$  ceramic system, using an indentation technique. A comparison revealed that the calculated stresses were appreciably larger than the measured surface stresses, indicating an important difference between the bulk and surface residual stresses. However, it was also shown that porosity in the metal could plastically expand and permit substantial dilatational relaxation of the residual stresses. Conversely it was noted that pore clusters were capable of initiating ductile rupture, by means of a plastic instability, in the presence of appreciable tri-axiality. The role of ceramics for packaging of microelectronics will continue to be extremely challenging.

## I. Introduction

A number of applications in microelectronics involve combinations of metal and ceramic constituents. These constituents are typically subject to residual stress due to thermal expansion mismatch. The residual stresses may result in cracks, which impede the electrical performance of the device <sup>(1)</sup>.

There is a need for an alumina-based ceramic powder sinterable between 900 °C and 1200 °C for substrate applications in the electronics industry. This particular firing-temperature range permits the use of screen-printed metallization made from conventional electrically conductive metals (e.g. Cu, Ni) in co-fired systems <sup>(2)</sup>. The firing temperature of  $\text{Al}_2\text{O}_3$  is reduced with the addition of  $\text{SiO}_2$ . Sub-micrometer, mono-sized, and uniformly packed particles provide maximum driving force for homogeneous sintering throughout a sample <sup>(3)</sup>. Optimum compaction of the powder reduces the probability of voids. To make a composite ceramic of  $\text{Al}_2\text{O}_3$  and  $\text{SiO}_2$ , it is important to prepare a powder having individual particles of the chemical composition of the final ceramic; the powder should be composed of mono-sized, composite particles <sup>(4)</sup>. The goal of this article is to evaluate the residual stresses that develop (for a sample configuration) and to examine the implications for cracking.

## II. Experimental Part

$\text{Al}_2\text{O}_3$  particles dispersed in a solution of  $\text{pH} < 9$  have a positive electrostatic charge, and  $\text{SiO}_2$  particles dispersed in a solution of  $\text{pH} > 2$  have a negative charge (the isoelectric points of alumina and silica are 9 and 2, respectively). Thus, at pH levels between 2 and 9, a mixed colloidal dispersion of  $\text{Al}_2\text{O}_3$  and  $\text{SiO}_2$  may hetero-coagulate through mutual attraction by electrostatic forces to form a dispersion of composite particles <sup>(4)</sup>. If the silica particles are much smaller than the alumina particles, the latter will be covered with one or two layers of the former. The dispersion can then be sediment, centrifuged, or filter-pressed to obtain a uniform green compact for firing.

The  $\text{Al}_2\text{O}_3$  at a concentration of 0.4 mol/l, was ultrasonically dispersed in (water + isopropanol) = 1/1 to which acetic acid had been added to attain a pH of 3.5. The colloidal  $\text{SiO}_2$  was diluted to a concentration of 1.2 mol/l of solution in (water + ethanol) = 1/1 and sufficient acetic acid was added to match the pH of the alumina dispersion. Equal volumes of the two dispersions were prepared.

The alumina dispersion was then introduced at a rate of 3.5 ml/min into the vigorously stirred silica dispersion, allowing the alumina particles to become completely covered with silica particles. The composite colloidal dispersion was then centrifuged at 24.5 km/s<sup>2</sup>(2500 G) for 1hr and the supernatant containing the excess  $\text{SiO}_2$  particles was decanted. The remaining concentrated slurry was pressed at 34 MPa in a die set having two porous punches to obtain a green compact having a

relative density of 61%. Samples were fired in air at 900 ° to 1500 °C for 1 to 13 h; the relative linear shrinkage was measured with a dilatometer.

### III. Results and Discussion

The low-agglomerated composite powder obtained by the hetero-coagulation technique is shown in Fig.1a. Since the alumina dispersion was introduced slowly into the silica dispersion, virtually each alumina particle could be entirely converted with silica before encountering another alumina particle not yet covered with silica. In addition, an excess amount of silica was used so that all the alumina particles would be completely covered. These conditions were necessary to prevent extensive hetero-coagulation, the formation of large agglomerates ( $> 1 \mu\text{m}$ ) containing many  $\text{Al}_2\text{O}_3$  particles Fig.1b.

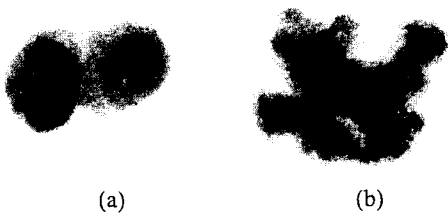


Fig.1. (a) 2 combined  $\text{Al}_2\text{O}_3$  particles coated with ultrafine  $\text{SiO}_2$  particles, (b) agglomerated particles

Specific surface areas, determined by single-point BET, were  $37 \text{ m}^2/\text{g}$  for the composite powder. Heat treatment in air to  $500^\circ\text{C}$  for 1 h removed essentially all of the water and organic compounds, as shown by differential thermal and thermo-gravimetric analyses. The heating rate was  $100^\circ\text{C}/\text{h}$  to avoid crack formation. A fracture surface of the unfired, compacted, composite powder (Fig.2) shows the packing uniformity attained using the slurry pressing technique. Samples of the  $\text{Al}_2\text{O}_3$  - $\text{SiO}_2$  compacts were fired in air at a constant heating rate of  $10^\circ\text{C}/\text{min}$ ; their respective relative linear shrinkages are given in Fig.3. These data confirm the enhanced sintering behavior of the composite  $\text{Al}_2\text{O}_3$  - $\text{SiO}_2$  powder. The chemical composition of the composite powder, 80wt%  $\text{Al}_2\text{O}_3$  and 20wt%  $\text{SiO}_2$ , was determined with an electron microprobe. This value corresponds to about two layers of  $0.02\text{-}\mu\text{m}$  spherical  $\text{SiO}_2$  particles covering the surfaces of  $0.3\text{-}\mu\text{m}$   $\text{Al}_2\text{O}_3$  particles. The composite powder reached a full density of  $3.4 \text{ g}/\text{cm}^3$  and HV hardness of  $1540 \text{ kg}/\text{mm}^2$  after firing for 1 h at  $1550^\circ\text{C}$ . As expected from the  $\text{Al}_2\text{O}_3$  - $\text{SiO}_2$  phase diagram <sup>(4)</sup>, the mullite phase ( $3\text{Al}_2\text{O}_3 : 2\text{SiO}_2$ ) formed at this temperature, giving the overall phase composition of 29 wt%  $\text{Al}_2\text{O}_3$  and 71 wt% mullite, as confirmed by X-ray diffraction. When the mullite phase formed, the sample expanded because of the slightly lower density of mullite compared to that of an equivalent mixture of alumina and Linear Relative

silica.

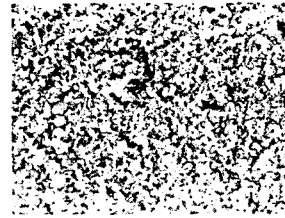


Fig.2. Fracture surface of green composite powder (bar =  $100 \mu\text{m}$ )

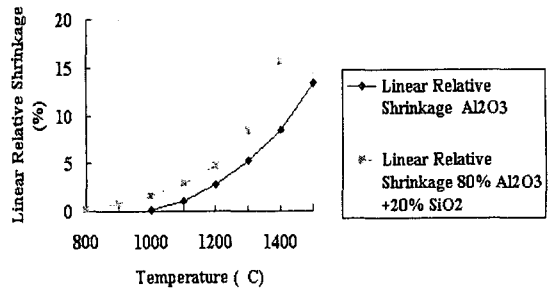
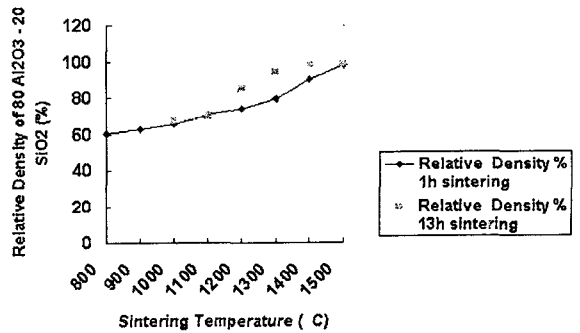
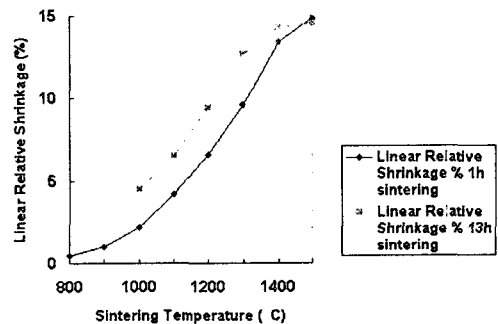


Fig.3. Sintering behavior of compacted 80 %  $\text{Al}_2\text{O}_3$  - 20 %  $\text{SiO}_2$  (1) and  $\text{Al}_2\text{O}_3$  (2) powders fired in air at  $10^\circ\text{C}/\text{min}$



(a)



(b)

Fig.4. Sintering behavior of 29 %  $\text{Al}_2\text{O}_3$  - 71 % mullite composite ceramics fired in air for 1 (a) and 13 h (b)

Differential thermal analysis indicated that the chemical reaction of mullite formation began at  $1490^\circ\text{C}$ . Figure 4 shows the relative densities obtained for the

composite powder compact after firing for 1 and 13 h at 900° to 1500 °C. The composite material had a relative density of 73% after firing for 1h at 1200 °C (Fig.5a) and 98 % after firing for 1 h at 1400 °C (Fig.5b); no grain growth was observed. Firing temperatures of 1125 and 1310 °C were required to give relative densities of 73% and 98%, respectively, after 13 h.

The metal constituent is generally amenable to plastic deformation and hence, the stress analysis is inherently an elastic/plastic problem. The residual stress is thus expected to exhibit dependence on the yield strength and work-hardening coefficient, as well as the mismatch in thermal expansion. However, the specific influence of these material variables on the residual stress depends on the configuration of the system. For present purposes, a cylindrical geometry is considered, as pertinent of the conduction element in a microelectronics package.

### Residual Stresses

Residual stresses are calculated for the cylindrical configuration, subject to the premise that processing is conducted at elevated temperatures, where the stresses are fully relaxed.

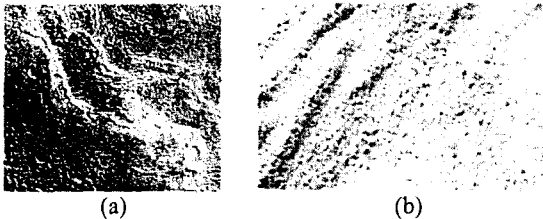


Fig.5. (a) Fracture surface of composite ( $\text{Al}_2\text{O}_3\text{-SiO}_2$ ) ceramics with 73 % dense sintered in air at 1200 °C for 1 h; (b) 98 % dense sintered in air at 1400 °C for 1 h

Stresses thus develop upon cooling due to thermal expansion mismatch. Specific stress amplitudes are computed using the material properties for the technologically significant system: copper/ $\text{Al}_2\text{O}_3$  ceramic. The calculations include considerations of temperature dependent plastic properties and of the influence of porosity, especially in the metal conducting element, on the residual stress. The residual stress computations are compared with experimental measurements obtained for the copper/ -  $\text{Al}_2\text{O}_3$ ,  $\text{SiO}_2$  ceramic system. The localized residual stresses are determined by indentation techniques, with indentations placed in the ceramic, adjacent to the metal/ceramic interface. The plastic properties of the metal required for stress determination are also assessed by indentation methods. With this technique, small Vickers indentations are placed in the ceramic, adjacent to the metal/ceramic interface. Then, the relative extensions of the radial cracks provide information pertinent to the sign and magnitude of the residual stress. Specifically, in the absence of residual stress, indentation at a load, P, creates a radial crack of radius, c, related to the toughness of the ceramic,  $K_c$ ,

$$K_c = \chi P(E/h)^{1/2} c^{-3/2} \quad (1)$$

where E and h are the modulus and hardness of the ceramic and  $\chi$  is a coefficient equal to 0.016. In the presence of residual stress, the crack length and geometry are modified, such that the residual stress,  $\sigma_R$ , and the crack radius, c, are related to the toughness by

$$K_c = \chi P(E/h)^{1/2} c^{-3/2} + \sigma_R \Omega c^{1/2} \quad (2)$$

where  $\Omega$  is a coefficient that depends on the uniformity of the residual fired (for a uniform field,  $\Omega = 2/\sqrt{\pi}$ ). The residual stress,  $\sigma_R$ , can be related to the metal/ceramic interface stress,  $\sigma$ , by

$$\sigma_R = \sigma(r/a)^2 \quad (3)$$

Hence, by first evaluating  $K_c$  from indentations placed at locations remote from the metal, the interface residual stress,  $\sigma$ , may be estimated from radial crack lengths measured at indentations placed at various radial positions, adjacent to the interface.

Inspection of cracking patterns around normal and longitudinal sections reveals that the circumferential or axial cracks are relatively enlarged, while the radially oriented cracks are suppressed. A condition of radial tension and circumferential compression is thus implied, consistent with the larger thermal expansion of the copper.

Determination of the toughness of the  $\text{Al}_2\text{O}_3\text{-SiO}_2$  ceramic from remote indentations indicates that  $K_c = 1.4 \text{ MPa m}^{1/2}$ . With this toughness, the interfacial residual tension can be determined from the radial crack lengths (as measured on the normal section) as  $\sigma = 130 \text{ MPa}$  ( $\chi = 0.009$ ).

### Flow Stress of Metal

The flow stress of the metal cylinder can also be estimated with indentation techniques. Data obtained by using included angles between 60° and 160° result in the flow stress trends summarized in Fig. 6.

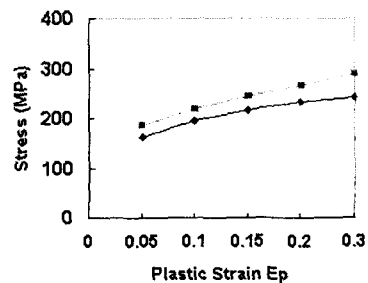


Fig.6. Stress-strain curves of copper alloys (Cu + x % Mullite Ceramics) obtained from indentation tests (1) x = 5 %; (2) x = 10 %; (3) x = 25 %

### Mechanical Damage

Two primary modes of damage have been observed in the copper/  $\text{Al}_2\text{O}_3\text{-SiO}_2$  ceramic system. Interface decohesion (Fig.7b) has been identified at a small

fraction of normal and longitudinal sections. Ductile fracture of the copper has also been detected (Fig.7c) at various axial locations. These modes of damage are induced by the tensile residual stresses in the radial and axial directions, respectively. Appreciable porosity is also observed throughout the copper phase.

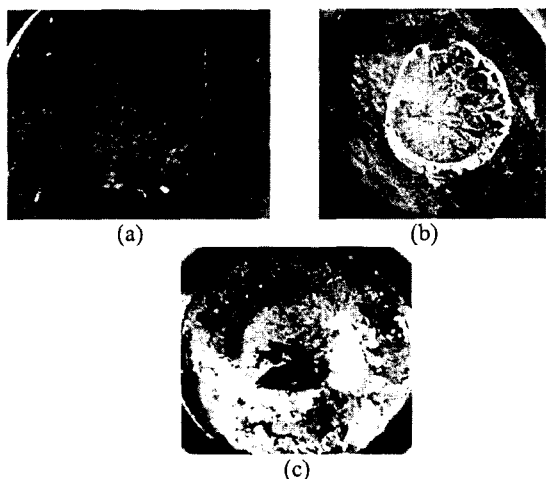


Fig.7 (a) Perfect bonding of metal/ceramics; (b and c) failure modes in metal / ceramics showing (b) interface decohesion; (c) ductile failure of metal

#### Remarks on Residual Stresses

The plastic flow properties of the copper measured at room temperature can be used in conjunction with the elastic properties of the copper and  $\text{Al}_2\text{O}_3 - \text{SiO}_2$  ceramic to compute the residual stresses. An interface residual stress,  $\sigma = 1500$  MPa is obtained. This stress is substantially in excess of the measured stress ( $\sigma = 130$  MPa), the residual stresses have been measured on the surface, where  $\sigma_z = 0$  applies. On the surface the stresses are determined exclusively by the plastic flow stress, as confirmed by the similarity in the present measurements of the residual stress and the plastic flow stress (Fig.6). However, the residual stress may also be appreciably less than the calculated stress of 1500 MPa, due to plastic dilatation of the pores in the copper (Fig.7). As estimated, porosity in excess of 0.01 can reduce the residual stress by a factor of  $\approx 8$ ; a reduction, which coincidentally results in a stress similar to the measured stress. It is thus concluded that porosity in the copper should allow appreciable relaxation of the residual stress. Initial porosity in the copper may also have the detrimental effect of inducing premature ductile rupture (Fig.7c). Void clusters are capable of initiating ductile rupture by means of a plastic instability<sup>(2-3)</sup>. The rupture strain depends on the initial fraction of voids and the triaxiality. Consequently, since the triaxiality is relatively large in this case,  $\sigma/\sigma_z = 0.67$ , premature ductile rupture would be encouraged by local void clusters in the copper. A homogeneous distribution of initial porosity in the copper is evidently needed to inhibit local ductile rupture, while still permitting stress relaxation.

#### IV. Conclusion

A stress analysis was conducted for a linear work-hardening metal cylinder embedded in an infinite ceramic matrix. The bond between the metal and ceramic is established at high temperature and stresses develop during cooling to room temperature. The calculations show that the stresses depend on the mismatch in thermal expansion, the elastic properties, and the yield strength and work-hardening rate of the metal. Experimental measurements of the surface stresses have also been made on a  $\text{Cu} / \text{Al}_2\text{O}_3 - \text{SiO}_2$  ceramic system, using an indentation technique. A comparison reveals that the calculated stresses are appreciably larger than the measured surface stresses, indicating an important difference between the bulk and surface residual stresses. However, it is also shown that porosity in the metal can plastically expand and permit substantial dilatational relaxation of the residual stresses. Conversely it is noted that pore clusters are capable of initiating ductile rupture, by means of a plastic instability, in the presence of appreciable triaxiality. A homogeneous distribution of porosity in the metal is needed.

#### REFERENCES

- [1] Electronic ceramics. Properties, Devices and Applications. Ed. by L. Levinson. NY, 1988
- [2] B. Schwartz, Microelectronics packaging, Bull Am. Ceram. Soc., V.63, 1984, pp.577-81
- [3] B. Schwartz, Review of multilayer ceramics for microelectronics packaging, J. Phys. Chem. Solida, V.45, 1984, pp. 1051-57.
- [4] N. Korobova, The metal alkoxides as source materials in the sol-gel technique. Book 1. "Alumina - Silicate sol-gel materials: ceramics and thin films", Almaty, 1997.